Supplementary Information

Halogen-Bonded Self-Assembly of Mononuclear Lanthanide (III) Complexes: Variable Temperature Photoluminescence Study and Sensing of Picric Acid

Anil Rajnath Singh,[a] Arnab Sil,[b] Kumar Shivam,[a] Vishnu Poonia,[b] Simran Thakur,[c] Biswa Prakash Nayak,[c] Hatem M. Titi, *[d] Biswajit Guchhait, *[b] Ranjan Patra*[a]

[a]*Amity Institute of Click Chemistry Research & Studies (AICCRS), Amity University, Noida, India. Email: rpatra@amity.edu*

[b]*Department of Chemistry, School of Natural Sciences, Shiv Nadar University, Dadri, Uttar Pradesh – 201314, India. Email: biswajit.guchhait@snu.edu.in*

[c]*Amity Institute of Forensic Science (AIFS), Amity University, Noida, India.*

[d]*Department of Chemistry McGill University 801 Sherbrooke St. West, Montreal, QCH3A0B8, Canada.*

Experimental section:

Materials

General materials and methods: The solvents and other general reagents used in this work were received from commercial sources and used without further purification. $Dy(NO_3)_3 \cdot xH_2O$, $Sm(NO_3)_3 \cdot 6H_2O$, $Gd(NO_3)_3 \cdot 6H_2O$ were obtained from the Sigma Aldrich Chemical Co. (U.S.A.) and used as obtained. Ligand 2-Bis(2-hydroxy-3,5-dibromo benzyl)aminomethyl]pyridine was synthesized according to the literature procedure.

Physical Measurements

UV-Vis spectra were recorded on a Perkin Elmer UV-Vis spectrometer. IR spectra were recorded on a Bruker Tensor 27 system spectrophotometer in ATR mode. Powder X-ray Diffraction (PXRD) was measured by a XEUSS SAXS/WAXS system by Xenocs, operated at 50 kV and 0.60 mA. The X-ray radiation collimated with FOX2D mirror and two pairs of scatter slits from Xenocs.

The data were collected in the transmission mode geometry using Cu*K*α radiation (wavelength λ = 1.54 Å), Mass spectra was recorded in ESI (Negative mode)

General synthesis of $[LnL_2][Et_3NH]$.THF/H_2O (Ln = Dy, Sm and Gd) (H_2L = 2-Bis(2-hydroxy-3,5 dibromo benzyl)aminomethyl]pyridine);
2-Bis(2-hydroxy-3,5-dibromo benzyl)aminomethyl]pyridine (H_2L) (63.5 mg, 0.1 mmol) was dissolved in 10 ml dichloromethane. 3-4 drops of triethylamine were added. The mixture was stirred to get a clear solution. Methanolic solution of lanthanum nitrate hexahydrate $M(NO_3)_3$.6H2O (0.1 mmol) was prepared and added to the ligand solution. The stirring was continued for 6 hours. After that, the solvent was removed in a rotary evaporator to get the solid complex, which was further washed with hexane. Then the solid was redissolved in tetrahydrofuran. The solution was layered with acetonitrile in the crystallization tube and left for slow evaporation. After 6-7 days colourless crystals of complexes were obtained.

Complex 1: H_2L (63.5 mg, 0.1 mmol) and $Dy(NO_3)_3$.6H2O (43.8 gm 0.1 mmol) Yield: 0.068 g, 44.5% (based on ligand). IR (KBr ν/cm-1): 3545.4(br), 3024.8(br), 2726.6(m), 1648.4(m), 1544.6(m), 1522.9(m), 1483.5(s), 1324.5(s), 1228.3(s), 1143.5(s), 1032.4(s), 1062.5(s), 946.3(w), 878.6(w) 862.7(m), 724.3(s), 624.4(m), 612.8(m),584.6 (m), 532.3(m). UV-Vis (DCM, λmax): 254 nm, 314 nm, m/z= 1429.4806 (ESI-)

Complex 2: H_2L (63.5 mg, 0.1 mmol) and $Sm(NO_3)_3$·5H2O (41.4 gm 0.1 mmol) Yield: 0.077 g, 48.5% (based on ligand). IR (KBr ν/cm-1): 3587.5(br), 3124.8(br), 2772.6(m), 1662.47(m), 1546.6(m), 1505.9(m), 1448.5(s), 1364.5(s), 1248.3(s), 1152.5(s), 1062.4(s), 1028.5(s), 965.3(w), 868.6(w) 824.7(m), 769.3(s), 683.4(m), 612.8(m),552.6 (m), 512.3(m). UV-Vis (DCM, λmax): 232, 262 nm, 312 nm, m/z= 1419.4724 (ESI-)

Complex 3: H_2L (63.5 mg, 0.1 mmol) and $Gd(NO_3)_3$·5H2O (41.4 gm 0.1 mmol) Yield: 0.077 g, 48.5% (based on ligand). IR (KBr ν/cm-1): 3587.5(br), 3124.8(br), 2772.6(m), 1662.47(m), 1546.6(m), 1505.9(m), 1448.5(s), 1364.5(s), 1248.3(s), 1152.5(s), 1062.4(s), 1028.5(s), 965.3(w), 868.6(w) 824.7(m), 769.3(s), 683.4(m), 612.8(m),552.6 (m), 512.3(m). UV-Vis (DCM, λmax): 232, 262 nm, 312 nm, m/z= 1425.4835 (ESI-)

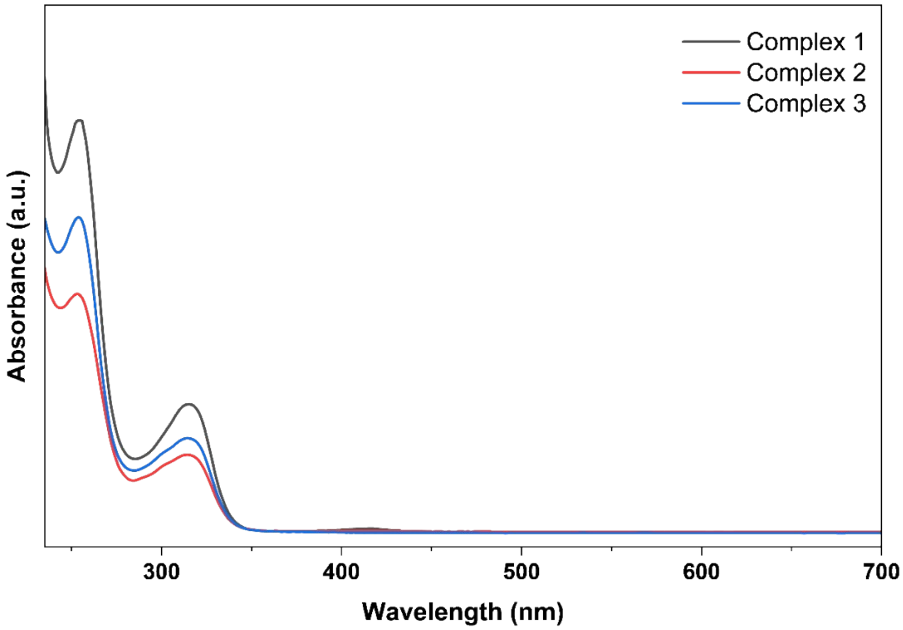

Figure S1. Overlaid UV–Vis spectra of complexes **1**, **2** and **3** in DCM at 298K

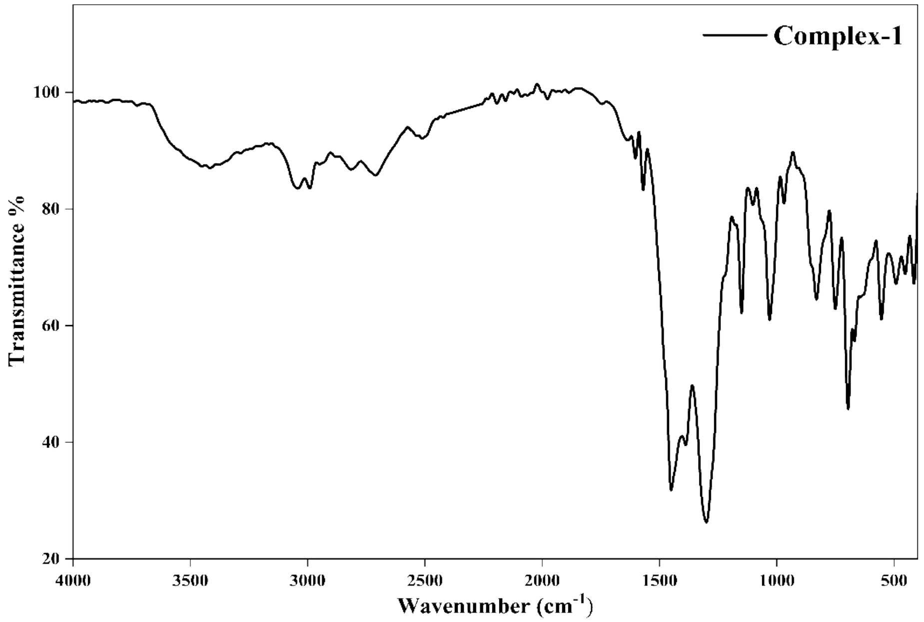

Figure S2. IR spectra of **1** at 298K

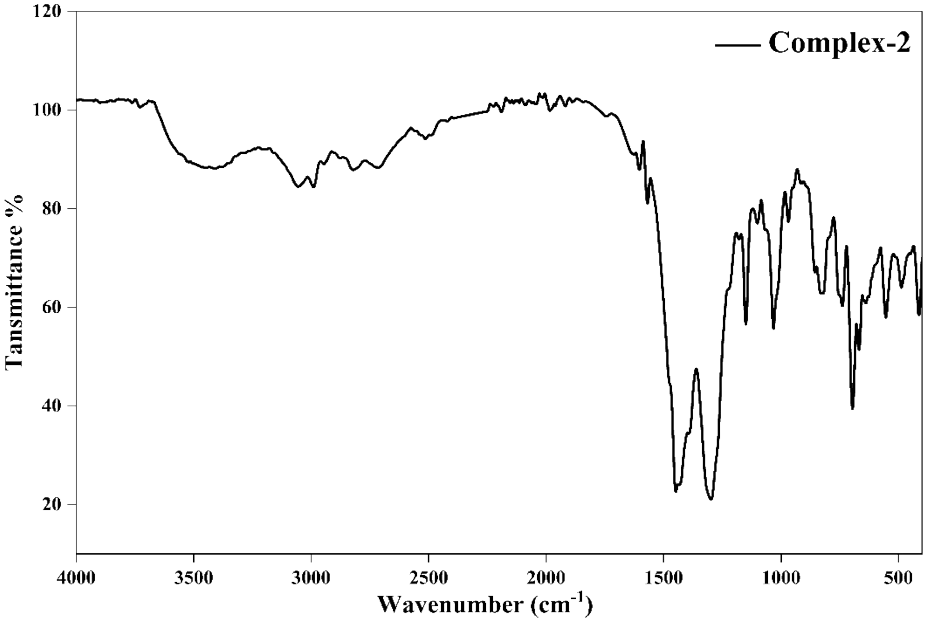

Figure S3. IR spectra of **2** at 298K

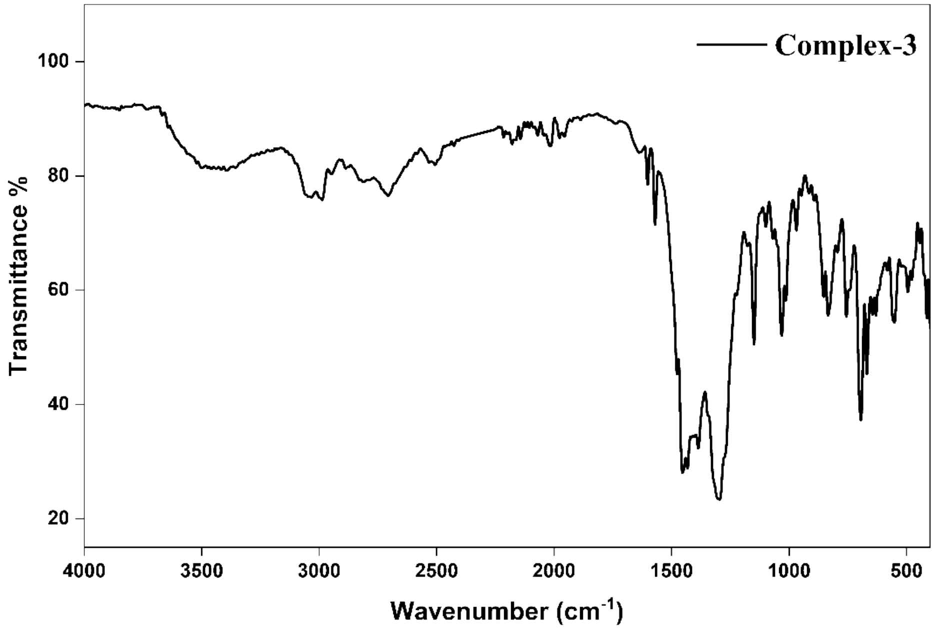

Figure S4. IR spectra of **3** at 298K

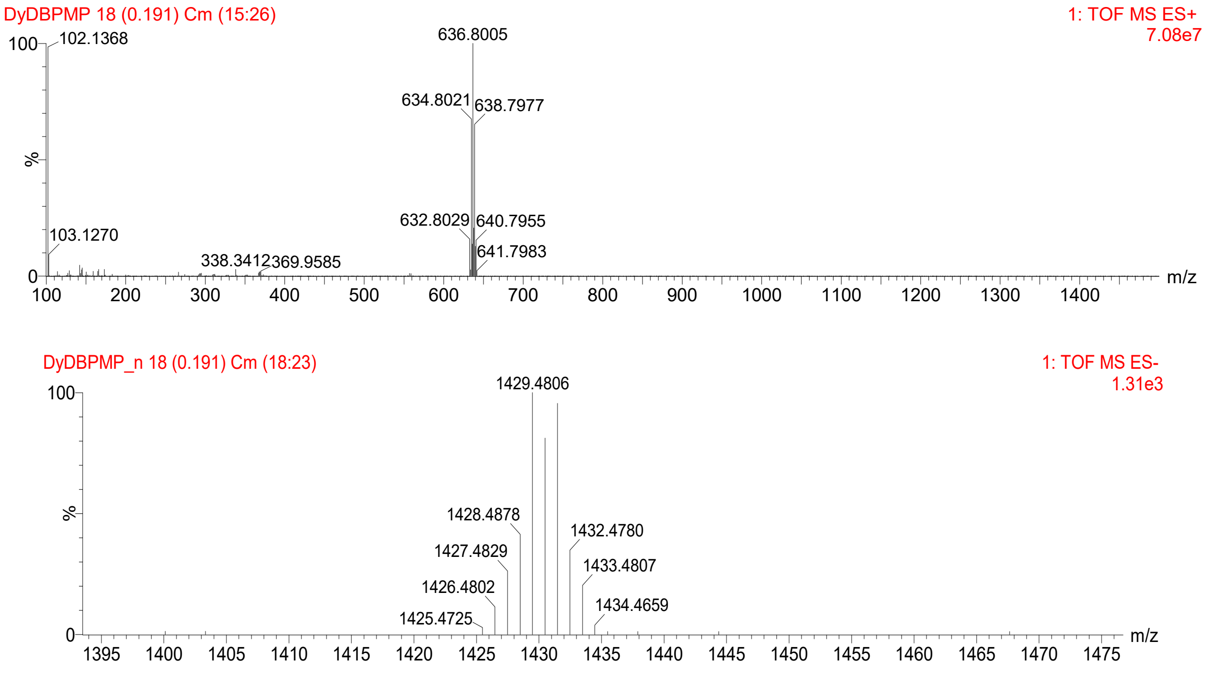

Figure S5. ESI–MS spectrum of **1** in positive and negative ion mode

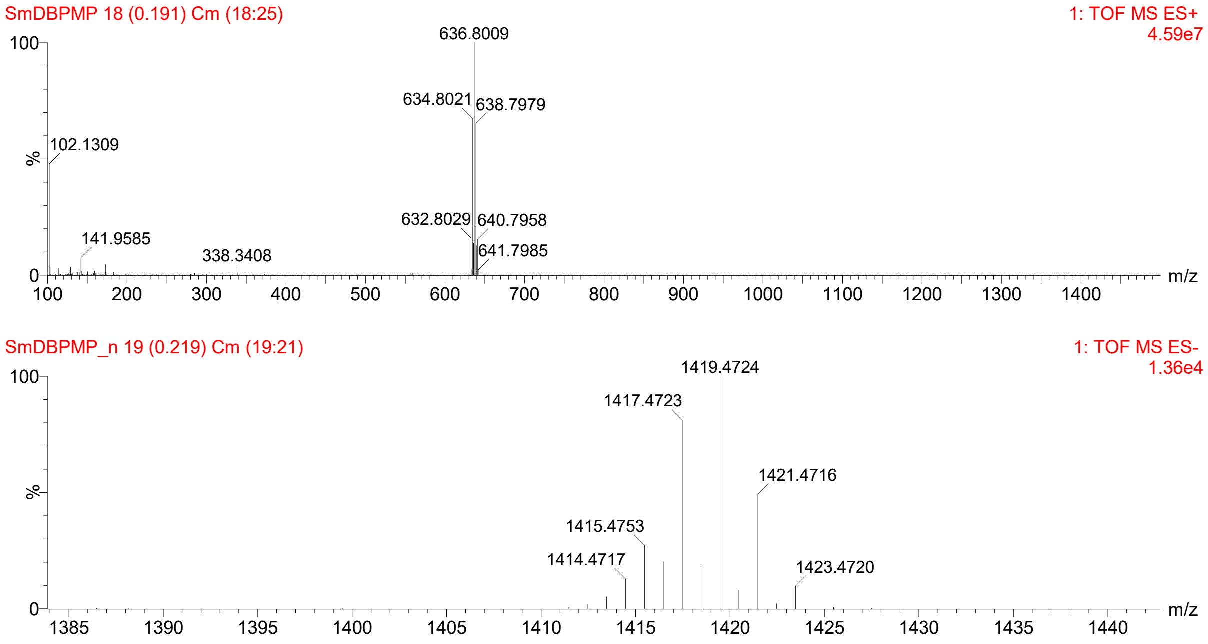

Figure S6. ESI–MS spectrum for **2** in positive and negative ion mode

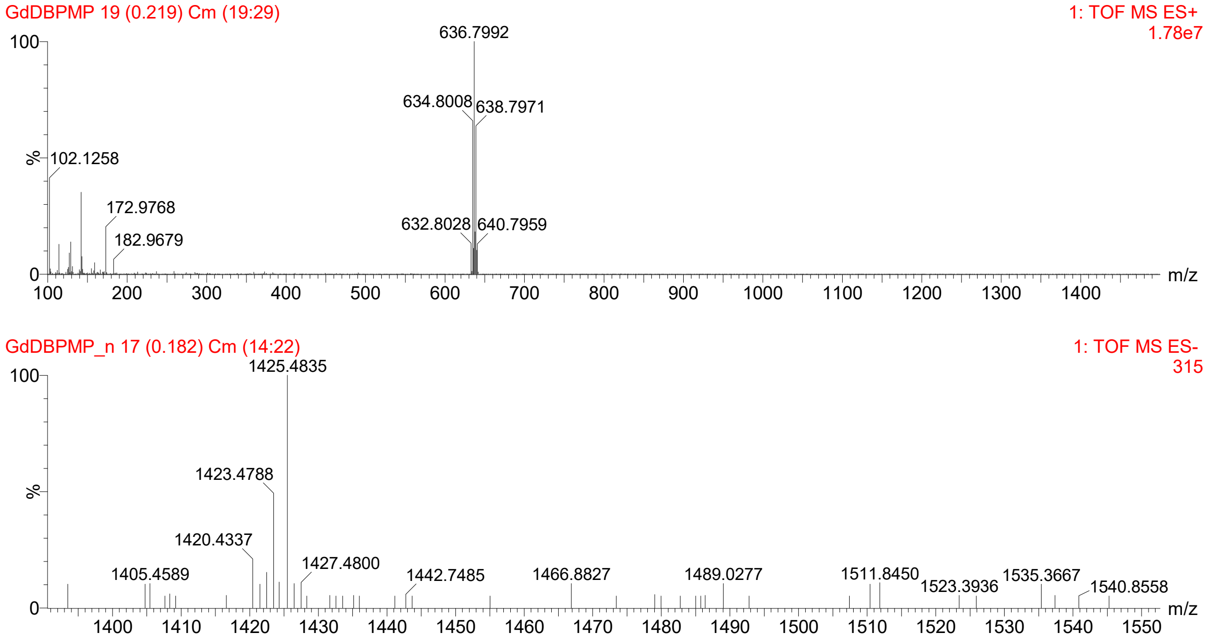

Figure S7. ESI–MS spectrum of **3** in positive and negative ion mode.

Table S1. Crystal data and data collection parameters of complex **1-3**

CCDC Number	2526623	2526622	2526624
Empirical formula	$C_{40}H_{28}Br_8DyN_4O_4$ + cation	$C_{40}H_{28}Br_8SmN_4O_4$ + cation	$C_{46}H_{46}Br_8GdN_5O_5$
Formula weight	1532.64	1520.49	1545.41
Temperature/K	293(2)	293(2)	296(2)
Crystal system	Monoclinic	Monoclinic	Monoclinic
Space group	$P2_1/n$	$P2_1/n$	$P2_1/c$
a/Å	12.9133(8)	12.9486(7)	25.763(3)
b/Å	20.2301(10)	20.1751(12)	19.803(3)
c/Å	20.8833(11)	21.0921(10)	22.210(3)
α/°	90	90	90
β/°	101.169(6)	101.564(5)	114.170(3)
γ/°	90	90	90
Volume/Å^3	5352.2(5)	5398.2(5)	10338(2)
Z	4	4	8
ρ_{calc}g/cm^3	1.902	1.871	1.986
μ/mm^{-1}	7.405	7.046	7.516
F(000)	2939.0	2888.0	5928.0
2Θ range for data collection/°	6.296 to 45	6.25 to 46	4.464 to 51
Index ranges	$-16 \leq h \leq 16, -26 \leq k \leq 17, -26 \leq l \leq 26$	$-16 \leq h \leq 15, -26 \leq k \leq 25, -26 \leq l \leq 25$	$-34 \leq h \leq 34, -26 \leq k \leq 26, -29 \leq l \leq 22$
Reflections collected	40586	30731	215117
Independent reflections	6967 [R_{int} = 0.1581, R_{sigma} = 0.0815]	7409 [R_{int} = 0.1553, R_{sigma} = 0.1076]	19206 [R_{int} = 0.1386, R_{sigma} = 0.0753]
Data/restraints/parameters	6967/536/515	7409/536/514	19206/0/1177
Goodness-of-fit on F^2	1.041	1.046	1.067
Final R indexes [I>=2σ (I)]	R_1 = 0.0878, wR_2 = 0.2348	R_1 = 0.0778, wR_2 = 0.1903	R_1 = 0.0474, wR_2 = 0.0831
Final R indexes [all data]	R_1 = 0.1256, wR_2 = 0.2572	R_1 = 0.1232, wR_2 = 0.2115	R_1 = 0.0963, wR_2 = 0.0993
Largest diff. peak/hole / e Å^{-3}	2.48/-1.81	0.92/-0.83	2.31/-1.25

Table S2: Selected Bond distance and Angle for complex-1

Bond distance (Å)	
Dy01- O00A	2.317(9)
Dy01-O00B	2.261(9)
Dy01-O00C	2.248(8)
Dy01-O00D	2.308(9)
Dy01-N00E	2.659(10)
Dy01-N00F	2.579(9)
Dy01-N00G	2.679(10)
Dy01-N00J	2.583(10)

Selected Bond Angle (°)	
O00A-Dy01-N00E	143.0(3)
O00A-Dy01-N00F	77.5(3)
O00A-Dy01-N00G	72.9(3)
O00A-Dy01-N00J	73.6(3)
O00B-Dy01-O00A	94.9(3)
O00B-Dy01-O00D	144.9(3)
O00B-Dy01-N00E	74.2(3)
O00B-Dy01-N00F	78.5(3)
O00B-Dy01-N00G	73.5(3)
O00B-Dy01-N00J	139.3(3)
O00C-Dy01-O00A	143.6(3)
O00C-Dy01-O00B	93.8(3)
O00C-Dy01-O00D	94.6(4)
O00C-Dy01-N00E	73.2(3)
O00C-Dy01-N00F	139.0(3)
O00C-Dy01-N00G	75.8(3)
O00C-Dy01-N00J	76.9(3)
O00D-Dy01-O00A	98.4(3)
O00D-Dy01-N00E	75.8(3)
O00D-Dy01-N00F	73.0(4)
O00D-Dy01-N00G	141.6(3)
O00D-Dy01-N00J	75.8(4)
N00E-Dy01-N00G	132.9(3)
N00F-Dy01-N00E	65.8(3)
N00F-Dy01-N00G	136.7(3)
N00F-Dy01-N00J	133.2(4)
N00J-Dy01-N00E	136.4(3)
N00J-Dy01-N00G	65.8(3)

Table S3: Selected Bond distance and Angle for complex-**2**

Bond distance (Å)	
O0AA-Sm1	2.370(8)
O2AA-Sm1	2.320(8)
N0AA-Sm1	2.695(8)
O1AA-Sm1	2.293(8)
O3AA-Sm1	2.392(8)
N1-Sm1	2.617(10)
N4CA-Sm1	2.718(9)
N3-Sm1	2.664(9)

Selected Bond Angle (°)	
O0AA-Sm1-N0AA	143.1(3)
O0AA-Sm1-O3AA	97.4(3)
O0AA-Sm1-N1	77.7(3)
O0AA-Sm1-N4CA	73.4(3)
O0AA-Sm1-N3	73.1(3)
O2AA-Sm1-O0AA	143.9(3)
O2AA-Sm1-N0AA	72.9(3)
O2AA-Sm1-O3AA	94.0(3)
O2AA-Sm1-N1	138.4(3)
O2AA-Sm1-N4CA	76.1(3)
O2AA-Sm1-N3	76.5(3)
N0AA-Sm1-N4CA	134.3(3)
O1AA-Sm1-O0AA	96.8(3)
O1AA-Sm1-O2AA	92.6(3)
O1AA-Sm1-N0AA	75.2(3)
O1AA-Sm1-O3AA	145.9(3)
O1AA-Sm1-N1	79.5(3)
O1AA-Sm1-N4CA	73.6(3)
O1AA-Sm1-N3	137.4(3)
O3AA-Sm1-N0AA	74.9(3)
O3AA-Sm1-N1	73.4(3)
O3AA-Sm1-N4CA	140.4(3)
O3AA-Sm1-N3	76.6(3)
N1-Sm1-N0AA	65.5(3)
N1-Sm1-N4CA	137.3(3)
N1-Sm1-N3	134.5(3)
N3-Sm1-N0AA	136.0(3)
N3-Sm1-N4CA	63.9(3)

Table S4: Selected Bond distance and Angle for complex-**3**

Bond distance (Å)	
Gd1-N1	2.674(6)
Gd1-N2	2.594(6)
Gd1-N3	2.658(5)
Gd1-N4	2.582(6)
Gd1-O1	2.290(4)
Gd1-O2	2.282(5)
Gd1-O3	2.373(5)
Gd1-O4	2.269(5)
Gd1-N1	2.674(6)

-

Selected Bond Angle (°)	
N2-Gd1-N1	64.62(18)
N2-Gd1-N3	135.04(17)
N3-Gd1-N1	134.36(17)
N4-Gd1-N1	136.58(17)
N4-Gd1-N2	134.35(18)
N4-Gd1-N3	66.18(17)
O1-Gd1-N1	74.38(17)
O1-Gd1-N2	73.68(17)
O1-Gd1-N3	142.67(17)
O1-Gd1-N4	76.50(17)
O1-Gd1-O3	98.13(17)
O2-Gd1-N1	73.79(17)
O2-Gd1-N2	138.33(17)
O2-Gd1-N3	74.83(17)
O2-Gd1-N4	79.30(17)
O2-Gd1-O1	98.12(17)
O2-Gd1-O3	145.27(16)
O3-Gd1-N1	140.43(17)
O3-Gd1-N2	75.94(17)
O3-Gd1-N3	73.63(17)
O3-Gd1-N4	74.99(17)
O4-Gd1-N1	76.24(17)
O4-Gd1-N2	75.08(17)
O4-Gd1-N3	73.39(17)
O4-Gd1-N4	139.46(17)

O4-Gd1-O1	143.92(16)
O4-Gd1-O2	93.29(17)
O4-Gd1-O3	91.35(17)

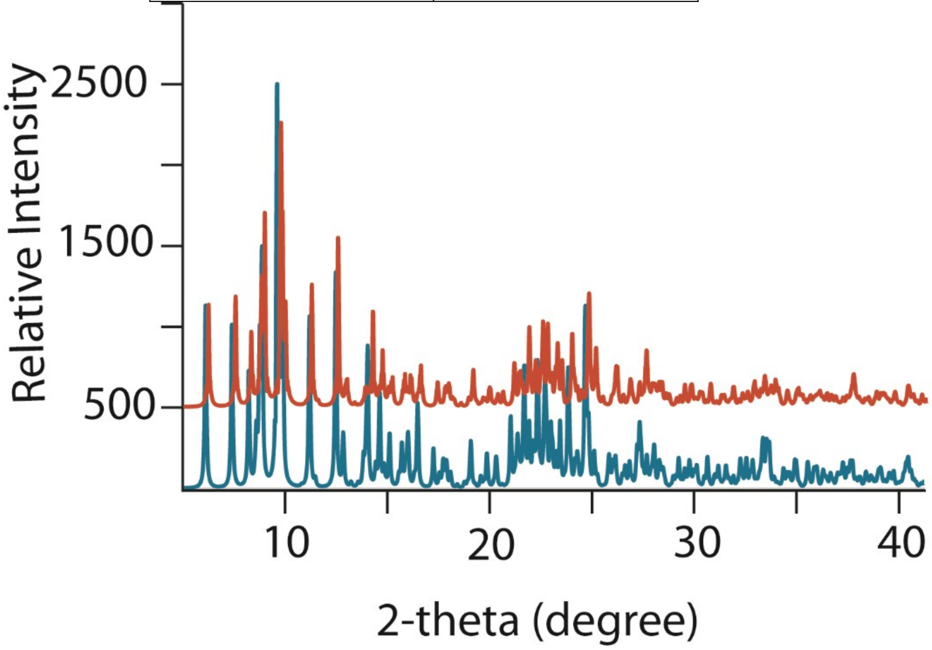

Figure S8. Overlapped PXRD pattern: experimental (red) and simulated (blue) [the pattern was generated using the CIF file in Mercury software] of **1** at 298K**.**

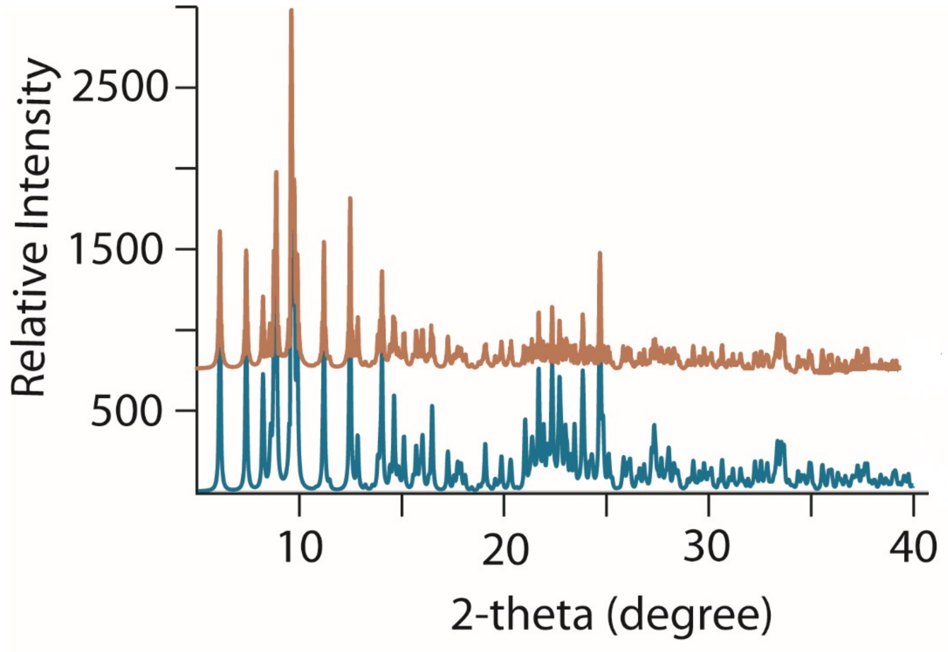

Figure S9. Overlapped PXRD pattern: experimental (red) and simulated (blue) [the pattern was generated using the CIF file in Mercury software] of **2** at 298K**.**

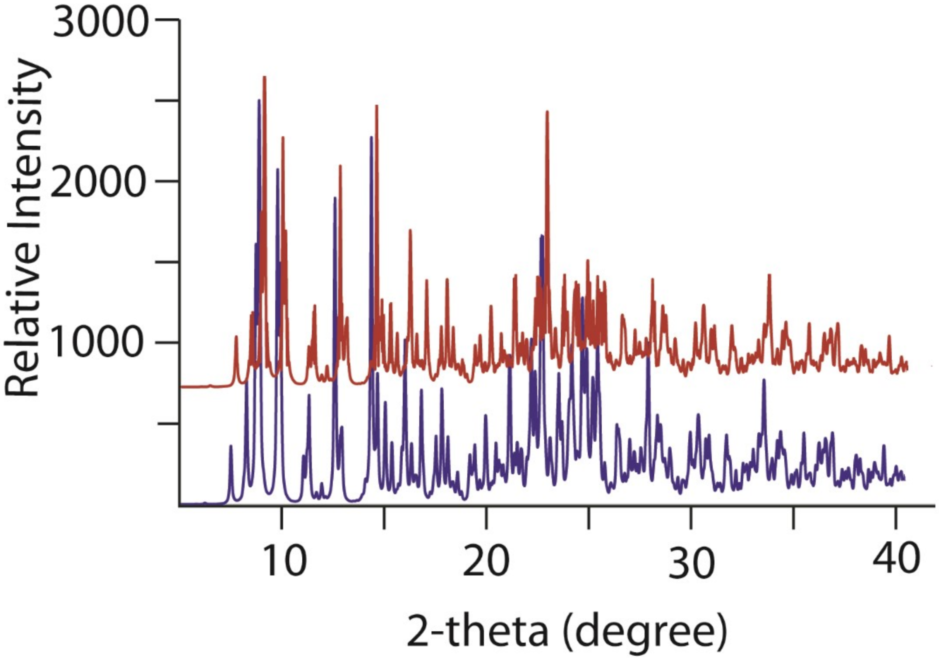

Figure S10. Overlapped PXRD pattern: experimental (red) and simulated (blue) [the pattern was generated using the CIF file in Mercury software] of **3** at 298K**.**

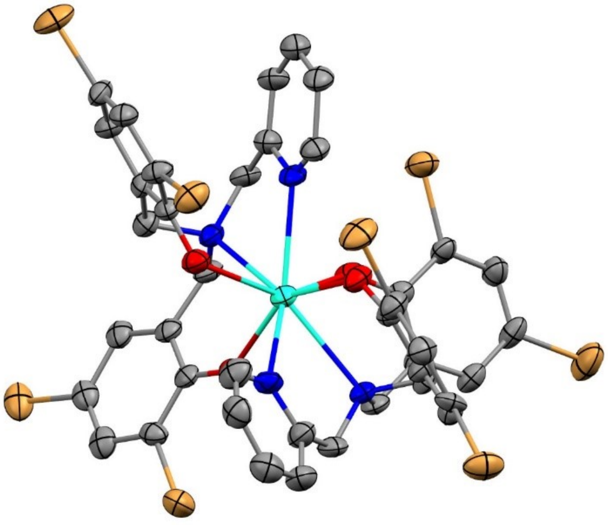

Figure S11. Perspective view of complex **1** showing 40% thermal ellipsoids for all non-hydrogen atoms at 293 K (H-atoms have been omitted for clarity).

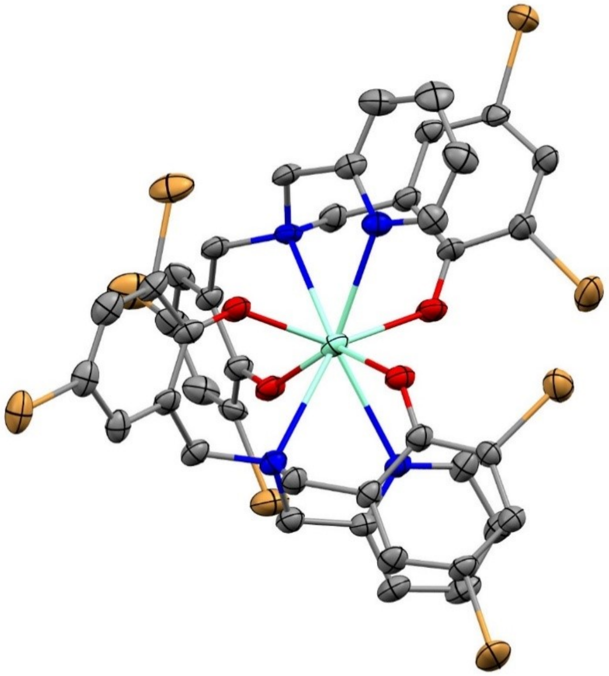

Figure S12. Perspective view of complex **2** showing 40% thermal ellipsoids for all non-hydrogen atoms at 293 K (H-atoms have been omitted for clarity).

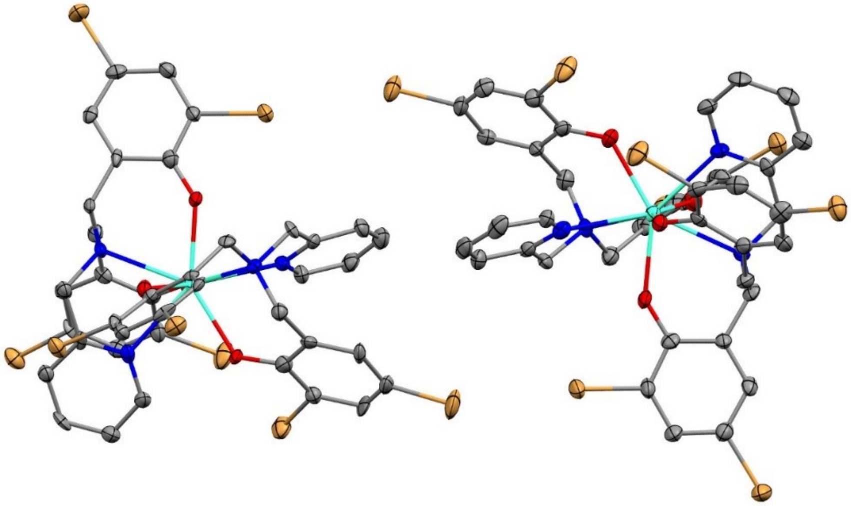

Figure S13. Perspective view of complex **3** showing 40% thermal ellipsoids for all non-hydrogen atoms at 293 K (H-atoms have been omitted for clarity).

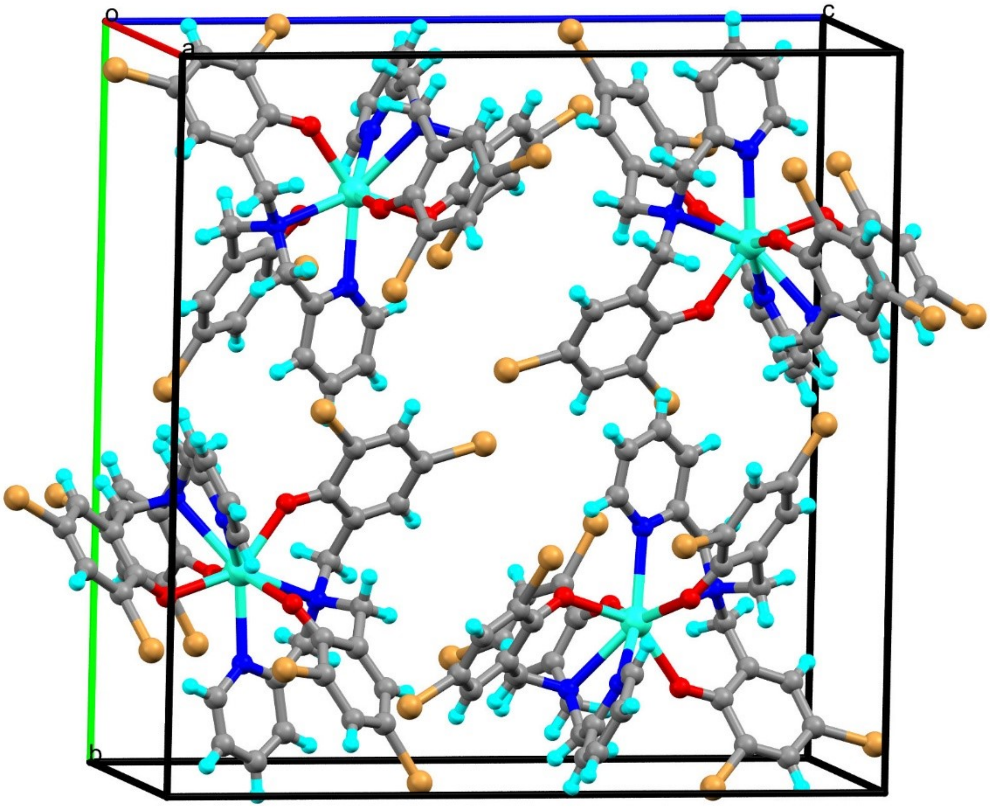

Figure S14. Packing diagram of the complex 1

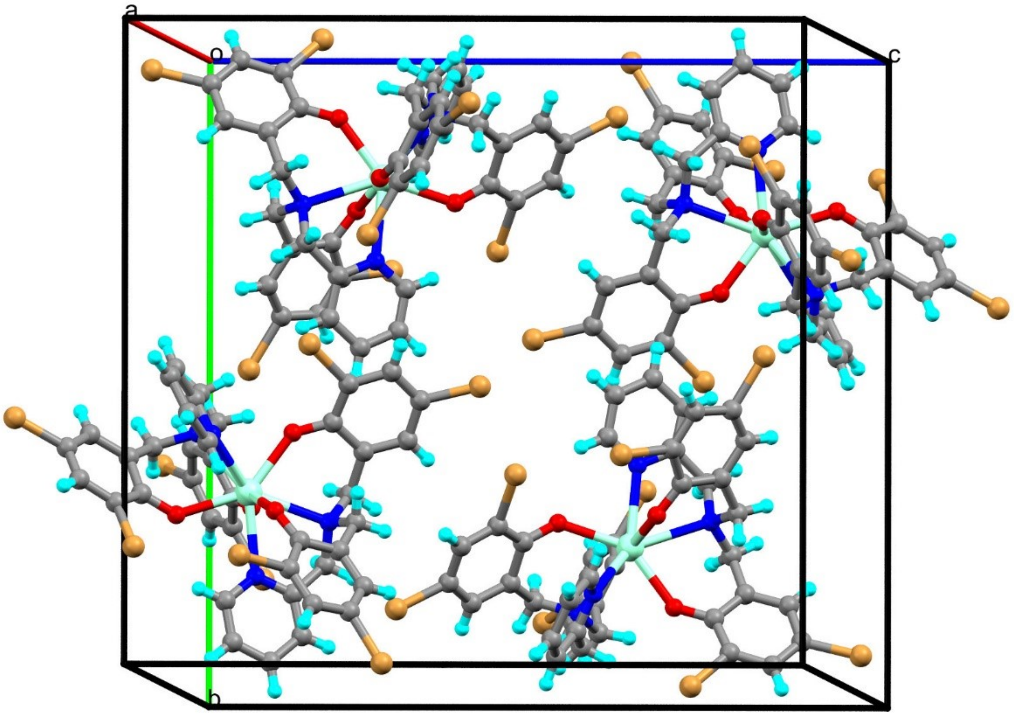

Figure S15. Packing diagram of the complex 2

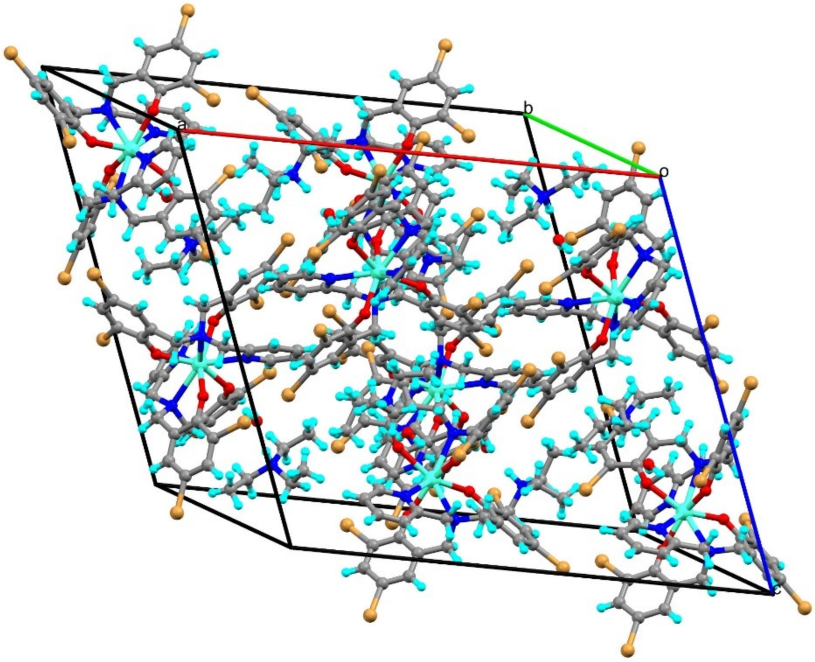

Figure S16. Packing diagram of the complex 3

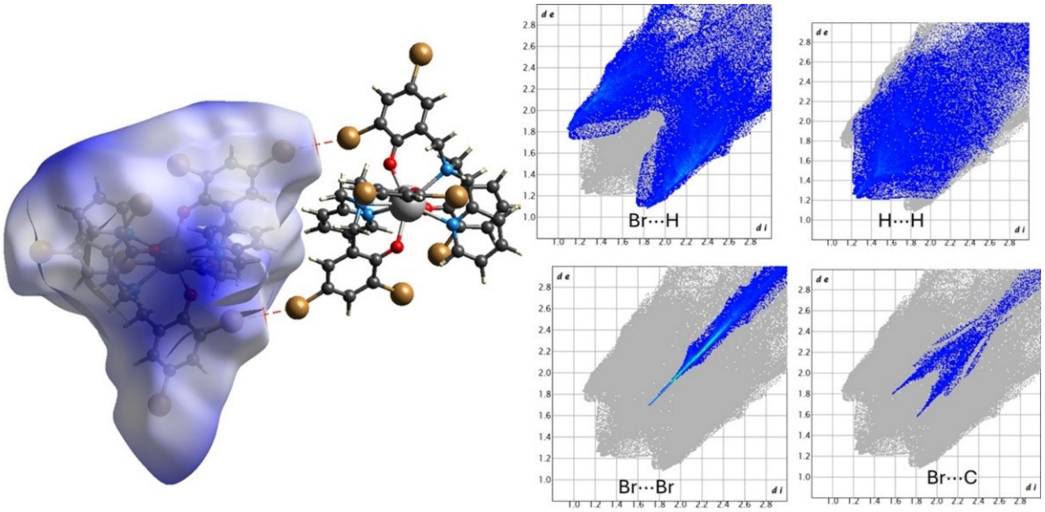

Figure S17: Calculated Hirshfeld surfaces (left) and relative contributions of various intermolecular contacts to the Hirshfeld surface (right) in complex **2**

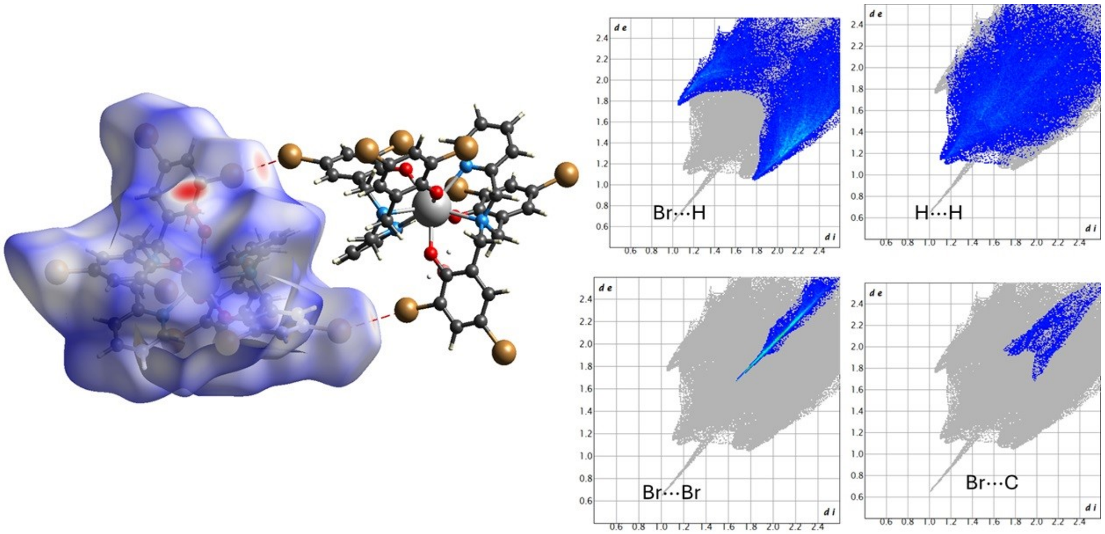

Figure S18: Calculated Hirshfeld surfaces (left) and relative contributions of various intermolecular contacts to the Hirshfeld surface (right) in complex **3**

Computational Details:

DFT calculations have been carried out by employing a B3LYP hybrid functional using, Gaussian 09, revision B.05, package.[1] Using the method of Becke's three-parameter hybrid exchange functional,[3] the nonlocal correlation provided by the Lee, Yang, and Parr expression,[2] and Vosko, Wilk, and Nussair 1980 correlation functional (III) for local correction. To reduce the paramagnetic effect on lanthanide metal we have replaced lanthanide by diamagnetic transition metal Cd. Geometry optimizations were performed. The basis set was LANL2DZ for the Cd-atom and 6-31G** for C, N, O, Br and H-atom. The coordinates are taken directly from the single-crystal X-ray data. Molecular electrostatic potential surfaces were calculated from optimized geometry.

References:

1. Gaussian 09, Revision A.1, M. J. Frisch, G. W. Trucks, H. B. Schle-gel, G. E. Scuseria, M. A. Robb, J. R. Cheeseman, G. Scal-mani, V. Barone, B. Mennucci, G. A. Petersson, H. Na katsuji, M. Caricato, X. Li, H. P. Hratchian, A. F. Izmaylov, J. Bloino, G. Zheng, J. L. Sonnenberg, M. Hada, M. Ehara, K. Toyota, R. Fukuda, J. Hasegawa, M. Ishida, T. Nakaji ma, Y. Honda, O. Kitao, H. Nakai, T. Vreven, J. A. Montgom-ery, J. E. Peralta, F. Ogliaro, M. Bearpark, J. J. Heyd, E. Brothers, K.N. Kudin, V. N. Staroverov, R. Kobayashi, J.

Normand, K. Raghavachari, A. Rendell, J. C. Burant, S. S. Iyengar, J. Tomasi, M. Cossi, N. Rega, J. M. Millam, M. Klene, J. E. Knox, J. B. Cross, V. Bakken, C. Adamo, J. Jaramillo, R. Gomperts, R. E. Stratmann, O. Yazyev, A. J. Austin, R. Cammi, C. Pomelli, J. W. Ochterski, R. L. Martin, K. Morokuma, V.G. Zakrzewski, G. A. Voth, P. Salvador, J. J. Dannenberg, S. Dapprich, A. D. Daniels, O. Farkas, J. V. For-esmanOrtiz, J. Cioslowski and D. J. Fox, Gaussian, Inc., Wallingford CT, (2009).

2. A. D. Becke, J. Chem. Phys., 1993, 98, 5648.
3. C. Lee, W. Yang and R. G. Parr, Phys. Rev. B, 1988, 37, 785.